Viscosity of particle laden films

Yousra Timounay[1,*] and *Florence* Rouyer[2,**]

[1] *Université Paris-Est, Laboratoire Navier (UMR CNRS 8205, École des Ponts ParisTech, IFSTTAR) 2, allée Kepler, 77420 Champs-Sur-Marne, France*
[2] *Laboratoire Navier, Université Paris-Est, Laboratoire Navier (UMR CNRS 8205, École des Ponts ParisTech, IFSTTAR), 5 bd Descartes, 77 454 Champs-Sur-Marne, France*

Abstract. We perform retraction experiments on soap films where large particles bridge the two interfaces. Local velocities are measured by PIV during the unstationnary regime. The velocity variation in time and space can be described by a continuous fluid model from which effective viscosity (shear and dilatational) of particulate films is measured. The 2D effective viscosity of particulate films η_{2D} increases with particle surface fraction ϕ: at low ϕ, it tends to the interfacial dilatational viscosity of the liquid/air interfaces and it diverges at the critical particle surface fraction $\phi_c \simeq 0.84$. Experimental data agree with classical viscosity laws of hard spheres suspensions adapted to the 2D geometry, assuming viscous dissipation resulting from the squeeze of the liquid/air interfaces between the particles. Finally, we show that the observed viscous dissipation in particulate films has to be considered to describe the edge velocity during a retraction experiment at large particle coverage.

1 Introduction

In many applications, as for example encapsulation or foams, hydrophobic particles are placed at liquid/air interfaces as they are expected to create an armor-like protective layer [1, 2]. Single liquid interfaces laden by hydrophobic particles, called particle rafts, are known to exhibit properties of both liquid interfaces and solid membranes [3, 4]. Such hybrid objects made of microscopic grains present size dependent properties as it is the case for granular media. A lot of studies are dedicated to the static regime and the Jansenn effect for example [5] of particle laden interfaces, whereas particulate soap films have been less studied [8]. In a previous study, we showed that the opening and retraction of particulate soap films depend on the particles position at the interfaces as well as on the constraints on the film edges [9]. Particles that bridge the two film's interfaces can inhibit the expansion of a hole because the rim formation and the opening of the capillary bridges between the grains are unfavorable. When the edge is constrained by a mobile stick, we observed a stationary regime during which the edge's velocity can be predicted at low particle surface fraction by a modified Taylor Culick model without any adjustable parameter. This model balances out surface tension that pulls the edge with the inertia of the collected particles. Larger is the particle surface fraction, lower is the retracting velocity. However, at larger particle surface fraction, experimental velocities are lower than expected, meaning that an additional resistive force slows down the particulate film retraction. We thus perform PIV measurements during the unstationary regime when surface tension accelerates the mobile stick to probe momentum diffusion and highlight the viscous character of particulate films.

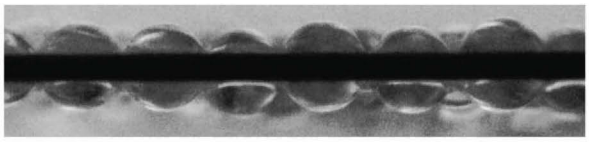

Figure 1. Side view of a particulate film, particle size $d = 250$ μm

2 Particulate films retraction experiment

Particulate films are created by pulling out a frame from a soap solution laden by hydrophobic particles at its liquid/air interface. The frame is a rectangle of 5 mm width noted a and 20 mm length. The soap solution is a Sodium Dodecyl Sulfate solution in water with a concentration close to the Critical Micellar Concentration 0.2% w/w and a density $\rho_l = 1000$ kg/m^3. The polystyrene beads are spherical and monodisperse, their diameter d can either be equal to 250 μm or 590 μm and their density $\rho_p = 1050$ kg/m^3. The contact angle between the particles and the liquid/air interface at equilibrium is equal to $95^o \pm 10^o$. Inside the film, the particles bridge the two interfaces, and the angle of contact is slightly deviated from its value at equilibrium (Figure 1).

*e-mail: yousra.timounay@ifsttar.fr
**e-mail: florence.rouyer@u-pem.fr

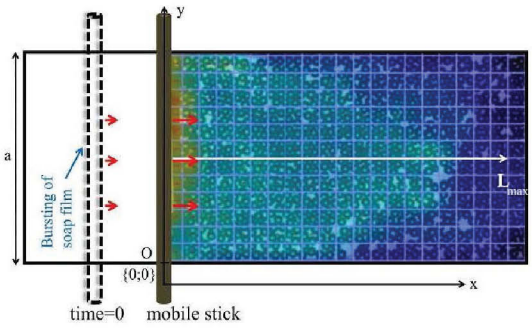

Figure 2. Sketch of the retracting film experiment with PIV image. The local velocities increase from blue to red.

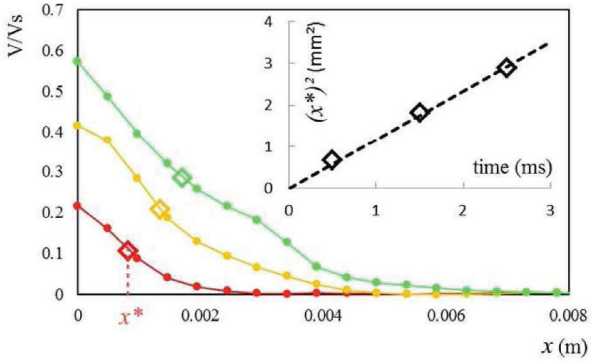

Figure 3. Velocity profiles as a function of the distance to the stick, 5 , 15 and 25 ms after the stick motion starts. Insert: square of distance for which velocity is half the velocity of the stick (diamonds in the main graph) versus time.

A mobile stick is placed at the surface of the horizontal frame, perpendicularly to the wires, to pull apart a particulate film and a bare film (Figure 2). The particle coverage ϕ of the film is calculated as $N\pi(d/2)^2/S$ where N is the number of particles present over a surface S of the covered film that corresponds to the area of the film after excluding the peripheral areas near the edges (we subtract $2d$ to the real width and length of the particulate film). The particles are counted by image analysis. Right after bursting the bare film on the left of the mobile stick, the stick is pulled by surface tension and accelerates. Motion propagates through the particulate film before the stick velocity reaches a stationary velocity noted V_s. Particle Image Velocimetry (PIV) allows to measure local velocity in the plane of the film (Figure 2) by comparing successive images taken by a fast camera placed above the retracting film. This technique requires to partition the images into small areas called interrogation regions. In our case, these areas are squares of two to three particle diameters side. PIV measurements we performed show that the local velocity varies essentially along the direction perpendicular to the stick (x-axis), whereas no variation is observed in the direction parallel to the stick (y-axis) except at the proximity of the wires. To get rid of these edge effects, we don't consider in the following the local velocities in the two squares along each of the wires perpendicular to the stick. In Figure 3, we plot the velocity averaged over y and normalized by V_s as a function of the distance to the mobile stick (x). The velocities $V(x,t)$ increase with time and decrease over a characteristic length that increases with time. We measured the distance at which the velocity is half the velocity of the stick and show that this distance varies as the square root of time (Figure 3-Insert). This behavior is characteristic of momentum diffusion i.e. viscosity. In the next section, a model for measuring effective viscosity from velocity profiles is presented.

3 Continuous model in 2D for effective viscosity measurements

A continuous model for 2D compressible viscous fluid is considered for modeling local velocities of particle laden films. Note that the particulate films have a constant mass while their surface is varying during experiments, so we assume that the corresponding 2D viscous fluid is compressible. The momentum equation is written in a mobile frame with the stick as the origin. As the compression is along the x-axis and since the velocity varies along this axis (we neglect velocity variation along y axis), the momentum equation is written as :

$$\frac{\partial V}{\partial t} + (V - V_{stick}(t))\frac{\partial V}{\partial x} = \nu\frac{\partial^2 V}{\partial x^2} \qquad (1)$$

where ν is the effective kinematic viscosity and $V(x,t)$ is the velocity of the particle laden film along x at a distance x from the stick and at a interval of time t from the beginning of stick motion i.e the film retraction.

The differential equation 1 is numerically solved assuming that the film is at rest initially, and assuming the continuity of velocities at the boundaries. These conditions can be written as : $V(x,0) = 0$, $V(0,t) = V_{stick}(t)$ and $V(L_{max},t) = 0$, where L_{max} is the distance from the stick to the opposite edge of the frame. The experimental velocity profiles are fitted by numerical solutions with only one adjustable parameter that equals the kinematic viscosity ν. Fits are shown in figure 4.

For films covered homogeneously with large particles bridging both interfaces as illustrated in figure 1, PIV measurements and velocity profiles analysis are done with particle coverage ϕ varied from 60% up to 84%. Moreover, few additional experiments are done for films with no large particles but tracers made of small polystyrene particles of diameter equal to 40 μm at small surface concentrations (less than 1%) that are positioned entirely inside the film. For these experiments with particle-free films, PIV measurements and velocity profiles analysis lead to a kinematic viscosity $\nu_0 \simeq 1.8 \,.\, 10^{-3}$ m^2/s. A dynamic 2D-viscosity η_{02D} is thus deduced considering a "2D density" for the liquid film that writes as $\rho_{02D} = \rho_l e$, where $e = 45$ μm is the liquid thickness of the particle-free film [9]. The calculated value $\eta_{02D} = \nu_0\rho_{02D} \simeq 7.9 \,.\, 10^{-5}$ Pa.s.m is in the order of the interfacial dilatational viscosity of the liquid/air interfaces that delimit the liquid film [10]. We thus highlight that the dominant source of dissipation is the de-

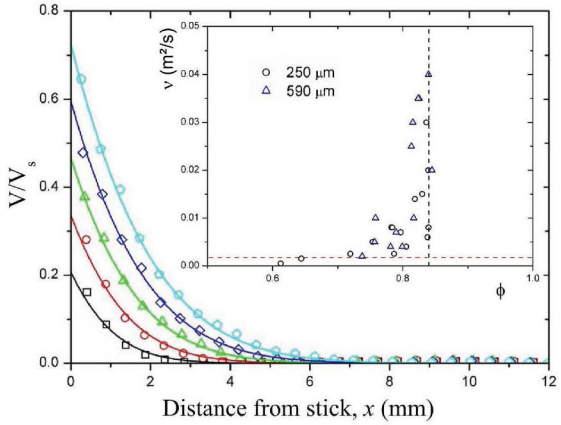

Figure 4. Velocity profiles as a function of the distance to the stick every 5 ms. The points are obtained from PIV measurements and the lines correspond to the numerical solutions of equation (1) for a particulate film where $d = 250\ \mu$ m and $\phi = 0.71$. Insert: the symbols correspond to the kinematic viscosity ν of particle laden films as a function of ϕ, the dotted horizontal and vertical lines correspond to $\nu_0 = 1.8\,.\,10^{-3}$ m^2/s and $\phi_c = 0.84$, respectively.

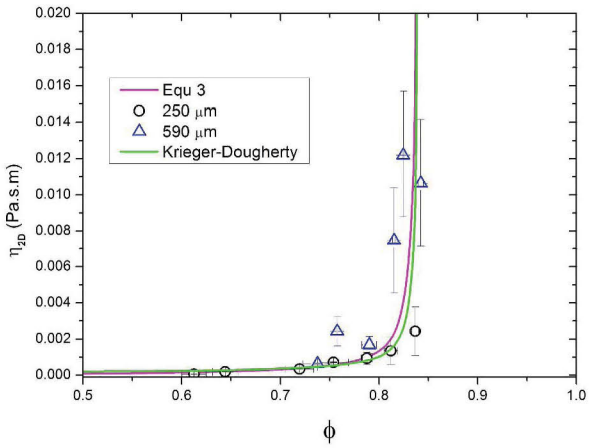

Figure 5. Effective dynamic viscosity versus particle surface fraction.

formation of the interfaces and not the deformation of the liquid inside the film.

4 Effective viscosity of particulate films: Results and Discussion

We now focus on the effective kinematic viscosity of the granular sheet and its variation with particle coverage. The effective kinematic viscosity of the granular sheet increases with particle surface fraction (figure 4-insert) from 10^{-3} to 4.10^{-2} m^2/s. These values are more than a thousand times the kinematic viscosity of water. At low ϕ, ν tends to the value ν_0 measured for particle-free films. The kinematic viscosity diverges at the critical packing fraction $\phi_c \simeq 0.84$ approaching jamming transition [11]. This critical behavior is also observed for drag friction that acts on a disk in a 2D dry granular medium [12]. Moreover, this divergence of viscosity is also characteristic of concentrated suspensions of hard spheres in a viscous liquid and indicates a transition from liquid-like behavior to solid-like behavior [13].

An effective dynamic 2D-viscosity η_{2D} is deduced from the kinematic viscosity as presented above for liquid films considering a "2D density" for particulate films $\rho_{2D} = (1-\phi)\rho_l e + \phi\rho_p \frac{2}{3}d$. The dependence of the effective dynamic 2D-viscosity with particle surface fraction is plotted in figure 5 and compared to "classical" laws for concentrated suspensions.

First, the experimental law of Krieger-Dougherty is tested : $\eta_{2D} = \eta_{02D}(1-\frac{\phi}{\phi_c})^{-k\phi_c}$ with $\eta_{02D} = 7.9\,.\,10^{-5}$ Pa.s.m, $\phi_c = 0.84$ and $k = 1$. This law has no adjustable parameter. Indeed, the values of ϕ_c and η_{02D} are justified previously. Moreover the value of $k = 1$ is consistent for $\phi \to 0$ with the model of Khair [14] in 2D that develops Einstein correction for the effective viscosity of dilute suspensions in a compressible fluid. This law is plotted in figure 5. Second, we adapt the 3D theoretical model of Mills for concentrated hard spheres [15] to the 2D geometry of the film. We write that the viscous dissipation of the particulate film $\frac{dE_v}{dt}$ per unit time and unit volume is due to viscous dissipation in the fluid film squeezed between the particles:

$$\frac{dE_v}{dt} \sim \eta_{2D}\dot{\epsilon}^2 \sim \eta_{02D}\left(\frac{\dot{\epsilon}d}{\Delta l}\right)^2 \omega \qquad (2)$$

where $\dot{\epsilon}$ is the average strain rate for the particulate film, $\Delta l = d\left(1-\sqrt{\phi/\phi_c}\right)$ is the average distance between the particles and $\omega = 2\phi\left(1-\sqrt{\phi/\phi_c}\right)$ is the surface fraction of the fluid. Equation 2 leads to an effective viscosity that diverges at ϕ_c and that writes :

$$\eta_{2D} \sim \eta_{02D}\frac{\phi}{1-\sqrt{\phi/\phi_c}} \qquad (3)$$

Equation 3 is plotted in figure 5 with the parameters fixed previously : $\phi_c = 0.84$, $\eta_{02D} = 7.9\,.\,10^{-5}$ Pa.s.m, and a prefactor of one-half.

The experimental data agree relatively well with both viscosity laws for concentrated 2D-suspensions presented above, this result suggests that the effective viscosity of particulate films is mainly due to the deformation of the liquid interfaces between the particles during the particulate film retraction.

Finally, we check if the effective viscosity presently measured is the source of dissipation responsible of the low retraction velocities measured at large particle coverage that are overestimated by the model based on the simple balance of inertia and surface tension. For this purpose, we calculate the viscous force per unit length F_η that the particulate film applies on the mobile stick during the film retraction at a time t_s when $V(0,t_s) = V_s$ (t_s corresponds to the end of acceleration of the stick and the beginning of the stationary regime):

$$F_\eta = \eta_{2D}\frac{e}{d}\left(\frac{\partial V}{\partial x}\right)_{(0,t_s)} \qquad (4)$$

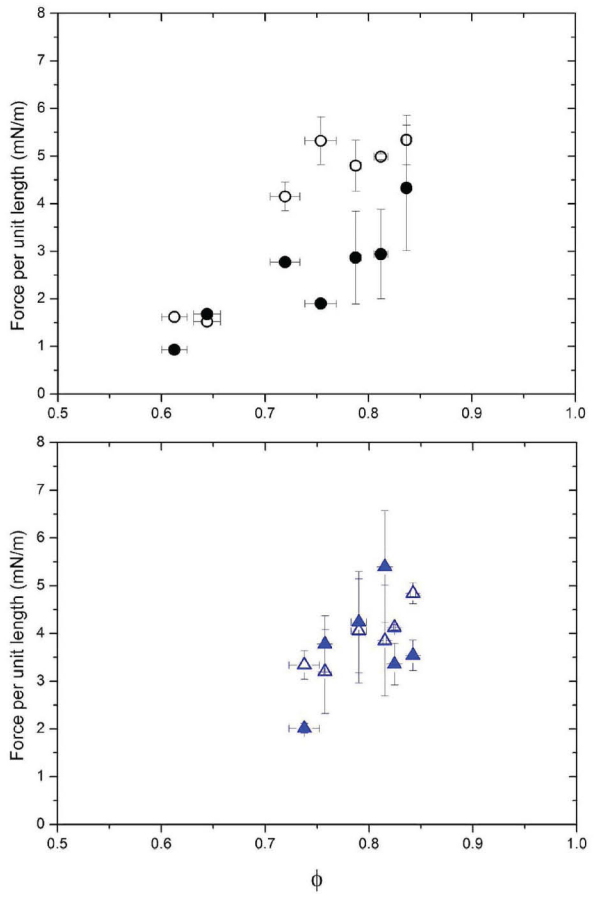

Figure 6. Open symbols and full symbols correspond to the resistive linear force F_r and to the linear viscous force F_η respectively. Particles diameter is equal to 250 μ m (top) and 590 μ m (bottom).

In figure 6, the force F_η is plotted versus ϕ. As expected, this force increases with particle coverage.

We now compare this force to the force F_r per unit length that resists the motion of the stick and that has to be added to the momentum balance on the stick to describe the stick motion during its stationary regime :

$$\beta\gamma - F - F_r = V_s \frac{dm}{dt} \tag{5}$$

Where $1 < \beta < 2$ because of the angle of the menisci that link the liquid film to the stick and $\beta\gamma - F$ is equal to the pulling force resulting from the surface tension of the two interfaces reduced by contact effects of the stick on the wires of the frames. Assuming that $\beta\gamma - F$ is similar in the case of particle-free films and particulate films, we deduce the value of F by measuring the retraction velocity of particle-free films. We find $F \simeq 10$ mN/m.

In figure 6, the linear force F_r is plotted versus ϕ, and compared to F_η. The two forces are quiet comparable. We thus conclude that viscous dissipation at the liquid interfaces that are highly solicited during particulate films retraction is responsible of the slowed down dynamics for particle surface fractions larger than 60%.

5 Conclusion

Retraction of particulate films where large particles bridge both interfaces is studied through a microscopic approach at the particles scale and a macroscopic one at the scale of the film. We show that such particulate films behave like a compressible viscous fluid which viscosity diverges approaching jamming transition. The 2D-effective viscosity of particulate films is comparable to viscosity model of hard sphere suspensions in 2D, suggesting that the dissipations result from the squeeze of the liquid bridges between the particles during a retraction experiment. The dissipations due to the interfacial dilatational viscosity of the liquid-air interfaces seems to be dominant relative to the dissipations in the bulk of the liquid connecting the particles. Moreover, the divergence of the effective viscosity at 0.84 that corresponds to the jamming surface fraction of a 2D granular media can be seen as a manifestation of the granular character of particulate films we present in this article.

Acknowledgments

We thank X. Chateau and O. Pitois for discussions. We acknowledge J.Bico for welcoming us in his laboratory for complementary experiments. We are grateful to IFSTTAR for financial support, and Judith Vatteville from LaVision for technical help.

References

[1] Aussillous, P. and Quere, D., Nature, **411**, 6840, 924-927 (2001)
[2] Stocco, A. et al., Soft Matter, **7**, 2, 631-637, (2011)
[3] Vella, D., Aussillous, P., Mahadevan, L., EPL (Europhysics Letters), **68**, 212 (2004)
[4] Planchette, C., Lorenceau, E., Biance, A.-L., Soft Matter, **8**, 2444 (2012)
[5] Cicuta, P., Vella, D., Physical review letters, **102**, 138302 (2009).
[6] Abkarian, M., et al. Phys. Rev. Lett. **99**, 188301 (2007)
[7] Pitois, O., Chateau, X., Eur. Phys. J. E, **38**:48 (2015)
[8] Horozov, T.-S., Current Opinion in Colloid & Interface Science, **13** 134–140 (2008)
[9] Timounay, Y., Lorenceau, E., Rouyer, F., EPL (Europhysics Letters), **111**(2), 26001 (2015)
[10] Kao,R., Edwards,D., Wasan, D., Chen, E., J. Colloid Interface Sci., **148**(1), 247–256 (1992)
[11] Majmudar, T. S., Sperl, M., Luding, S., Behringer, R. P., Physical Review Letters, **98**(5), 058001 (2007)
[12] Takehara, Y., Okumura, K., Phys. Rev. Lett. **112**,148001 (2014)
[13] Krieger, I. M., Dougherty, T. J., Transactions of The Society of Rheology, **3**, 1, 137-152 (1959)
[14] Khair, A.S., J. Colloid Interface Sci., **302**(2):702-3 (2006)
[15] Mills, P., Snabre, P., Eur. Phys. J. E, **30**, 309-316 (2009)